PREDICTING THE UNSTEADY PRESSURE ON A STREAMLINED BODY FROM ITS ACOUSTIC SIGNAL

S. M. Patrick * and H. M. Atassi †
University of Notre Dame
Notre Dame, Indiana USA

and

W. K. Blake [‡]
David Taylor Model Basin
C.D./N.S.W.C.
Bethesda, Maryland USA

ABSTRACT

The inverse aeroacoustic problem associated with a gust impinging on a flat-plate airfoil is formulated in terms of a Fredholm integral equation of the first kind. The feasibility of determining the unsteady pressure along the airfoil surface from the radiated acoustic signal is demonstrated. It is shown that the Hadamard conditions of existence and uniqueness of the inverse solution are satisfied, if the radiated sound is due to the gust interacting with the body. The third Hadamard condition for the continuous dependence of the solution on the input acoustic data shows the problem to be ill-posed. The singular value decomposition method with regularization is used to treat the associated illconditioned algebraic problem. Discretization and collocation techniques are used to represent the unsteady pressure on the airfoil. Both methods give very accurate reconstructions when "perfect" input data are used. The collocation method requires input from very few far-field locations, thus making it more suitable for applications. A sensitivity analysis based on the input data shows that the magnification of input error inherent in the inversion process can be controlled by the choice of the regularization parameter. A similar sensitivity analysis of the effect of mean-flow parameters, Mach number and reduced frequency, shows strong dependence of the inversion process on these parameters. suggesting the use of mid-field data for the inversion.

1. <u>INTRODUCTION</u>

The control and abatement of sound and vibration created by the interaction of nonuniform flows and solid bodies require a fundamental understanding of the interaction mechanism. One situation which has demanded much attention is the interaction of a streamlined body and a flow with vorticity. This situation is present in propellers, turbofans and guide vanes which often operate in the wake of other structural components. It occurs also in aircraft wings encountering atmospheric turbulence.

The traditional approach to quantifying the sound and

Fellow, Center for Applied Mathematics Professor Research Scientist vibration induced during such interactions has been to describe the upstream vortical flow and then to calculate the unsteady pressure induced on the blades and the far-field radiated sound. This is called the direct problem.

Whereas much has been learned about this interaction noise from the direct approach, an inverse approach is more applicable to the control of noise and vibration. In order to control noise and vibration, the origin of the phenomenon must be determined. One possible method for determining the origin of interaction noise is to calculate it from measurements of the sound created. This is called the inverse problem. For interaction noise, the inverse problem splits into two parts. The first part, the inverse aeroacoustic problem, consists of determining the unsteady pressure along the body from the far-field sound. In the second part, the inverse aerodynamic problem, the vortical disturbances in the flow are calculated using the unsteady pressure along the surface of the body. This paper focuses on the inverse aeroacoustic problem.

In the inverse aeroacoustic problem, the far-field unsteady pressure, or radiated sound, and the shape of the streamlined body are known. From this information, the unsteady pressure on the body must be calculated. If this calculation is possible, it could serve as a means for sensing in a control system and also it could be used to obtain unsteady surface pressure information which may be difficult to measure using standard measurement devices.

For most applications such as in aeronautics or propulsion systems, the structural components are designed to be streamlined bodies. The classical direct unsteady-aerodynamic treatments for such bodies uses linearized theory with the airfoil approximated by a flat plate. The classical treatment, in effect, uncouples the unsteady part of the solution from the mean flow, and brings about a significant simplification for the treatment of unsteady flows since the governing equation is reduced to a constant-coefficient convective wave equation. Although, more elaborate analytical and numerical methods have been developed to account for nonlinear effects associated with lifting airfoils, the linear theory gives good results for the gust problem of thin airfoils. [1]. In a similar fashion, it is believed that the

basic features of the inverse problem can be well understood by first examining the case of a flat-plate airfoil with its relatively simple mathematical formulation.

It is the intent of this paper to demonstrate the feasibility of the aeroacoustic inversion when the streamlined body is a flat-plate airfoil. The Hadamard criteria [2] of existence and uniqueness of a solution are considered first. For this problem both of these conditions are satisfied. Once existence and uniqueness are established, the challenge is to develop a method for performing the inversion accurately. We have found that the aeroacoustic inversion can be carried out using the method of singular value decomposition (SVD) with imbedded regularization techniques. The regularization techniques are necessary to handle the extreme sensitivity to errors in the input data. The paper will examine the level of accuracy associated with these methods in terms of the accuracy of far-field measurements and other input parameters.

2. MATHEMATICAL FORMULATION

Assuming there is an upstream imposed three-dimensional gust convected by a uniform flow where the fluid is inviscid, non-heat conducting, and compressible, and linearizing about the mean flow quantities, the governing equations are reduced to the linearized Euler equations. In the absence of incident acoustic waves, the unsteady flow field can be split into a potential or acoustic part and a rotational or vortical part which is convected by the mean flow [1]. In the linearized approximation, the mathematical problem can be reduced to a two-dimensional Helmholtz equation in the Prandtl-Glauert coordinate system [3] for a single Fourier component. The coordinate system and gust parameters are shown in Figure 1. The unsteady pressure is denoted as p'. The governing equation is given here in nondimensional form.

$$\left(\tilde{\nabla}^2 + K^2\right)P = 0\tag{1}$$

where

$$P(\tilde{x}_{1}, \tilde{x}_{2}) = p'e^{-i(k_{1}t + MK_{1}\bar{x}_{1} - \frac{k_{3}\bar{x}_{3}}{\beta})}$$

$$\tilde{x}_{1} = x_{1}$$

$$\tilde{x}_{2} = \beta x_{2}$$

$$\tilde{x}_{3} = \beta x_{3}$$

$$M = \frac{U_{\infty}}{c_{0}}$$

$$\beta = \sqrt{1 - M^{2}}$$

$$K_{1} = \frac{k_{1}M}{\beta^{2}}$$

$$K^{2} = K_{1}^{2} - \frac{k_{3}^{2}}{\beta^{2}}$$

The reduced frequency is $k_1 = \omega c/2U_{\infty}$, c_0 is the speed of sound, U_{∞} is the velocity of the free stream,

and $\tilde{\nabla}^2 = \frac{\partial^2}{\partial \tilde{x}_1^2} + \frac{\partial^2}{\partial \tilde{x}_2^2}$. Note that in this formulation, lengths are normalized with respect to the half chord, c/2, velocities with respect to U_{∞} , time with respect to $c/2U_{\infty}$, and unsteady pressure with respect to $a_2\rho_{\infty}U_{\infty}$ where a_2 is the amplitude of the vortical disturbance normal to the airfoil.

The equation relating the transformed unsteady pressure in the far-field and the transformed unsteady pressure on the airfoil follows from Green's theorem [3]. The relationship is

$$P(\vec{\tilde{x}}) = \frac{1}{2\pi} \int_{-1}^{1} \Delta P(\tilde{y}_1) \frac{\partial G_f(\vec{\tilde{x}}|\vec{\tilde{y}})}{\partial \tilde{y}_2} d\tilde{y}_1 \qquad (2)$$

where

$$G_f(\vec{x}|\vec{y}) = -\frac{i\pi}{2}H_0^{(2)}(K|\vec{y} - \vec{x}|)$$
 (3)

Here \vec{x} is the observation point and \vec{y} is the source point. Solutions to the inverse aeroacoustic problem will be obtained by solving this Fredholm integral equation of the first kind.

3. EXISTENCE AND UNIQUENESS

The inverse aeroacoustic problem is defined as determining the unsteady pressure on the flat-plate airfoil due to a vortical disturbance interacting with the airfoil from the resulting far-field acoustic signal. The existence criteria for this problem follows directly from the statement of the problem. The acoustic signal must be the result of the interaction of the vortical disturbance with the body. If there are spurious acoustics sensed by the measurement devices in the field, a reconstruction of the unsteady pressure on the body may not reflect only the response of the airfoil to the aerodynamic excitation. If the unsteady pressure on the airfoil represents an aerodynamic response, some information regarding its nature is already known from the direct problem; the unsteady pressure is characterized by a square root singularity at the leading edge and a Kutta condition at the trailing edge.

Once existence is established, uniqueness of the solution follows from properties of radiating solutions to the Helmholtz equation [4].

4. METHOD OF SOLUTION

4.1 General Techniques

Several methods for solving the integral equation (2) were tested. Each of the methods transformed the integral equation into a matrix equation of the form

$$\left[\begin{array}{c}A\end{array}\right] = \left[\begin{array}{c}\mathcal{M}\end{array}\right] \left[\begin{array}{c}B\end{array}\right] \tag{4}$$

For every method used, the matrix \mathcal{M} was ill-conditioned. Solutions to the matrix equation were

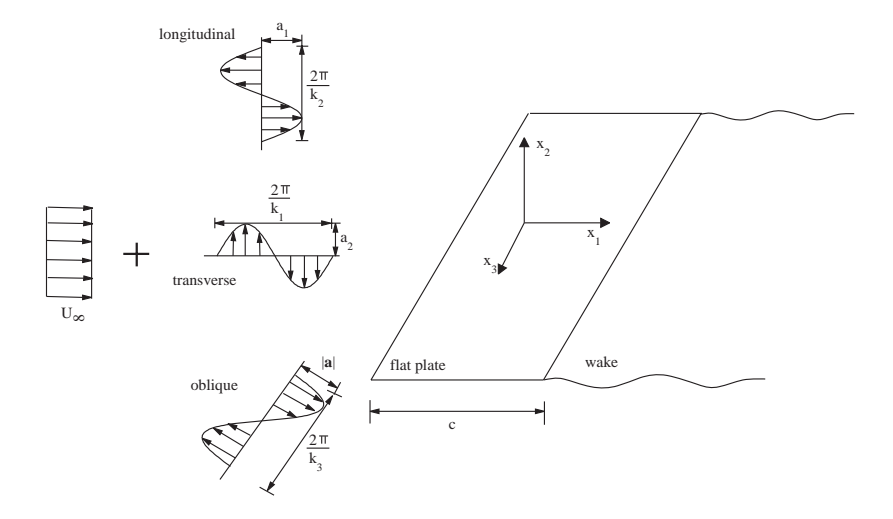


Figure 1: Flat-plate airfoil encountering three-dimensional vortical gust.

then obtained using optimization and regularization techniques. The optimization technique most commonly used to obtain solutions to ill-conditioned matrix equations is the the singular value decomposition (SVD). The premise for the SVD method is that a matrix \mathcal{M} of dimension $m \times n$ with $m \geq n$ can be represented as

$$\mathcal{M} = U\Sigma \overline{V}^t \tag{5}$$

where Σ is an $m \times n$ diagonal matrix with the first n diagonal terms containing the singular values, denoted here as σ_i , and the others containing zero, U is an $m \times m$ matrix containing the left singular vectors in its columns, and V is an $n \times n$ matrix containing the right singular vectors in its columns. Here the bar over V denotes the complex conjugate and the superscript t denotes the transpose. The columns of U, u_i , form a basis for the input space which contains A, and the columns V, v_i , form a basis for the reconstruction space which contains B. The solution to the matrix equation (4) then, is formed as follows

$$\left[\begin{array}{c}B\end{array}\right] = \sum_{i} \frac{\left[\begin{array}{ccc}A\end{array}\right] \cdot \left[\begin{array}{ccc}u_{i}\end{array}\right]}{\sigma_{i}} \left[\begin{array}{c}v_{i}\end{array}\right]$$
(6)

Further details on the SVD method as it applies to this problem are given in [4, 5].

When a matrix is ill-conditioned, the singular values decay to zero. In order to avoid dividing by these small values, regularization techniques are imbedded in the SVD method. One possible regularization technique is the spectral cut-off method where,, only a finite number of basis functions are used in the reconstruction. The number of basis functions used depends on how many singular values are greater than a certain cut-off value. Another regularization method, known as Tikhonov regularization [6] introduces a parameter α in Eq. (6). The solution is then modified to the form,

$$\begin{bmatrix} B \end{bmatrix} = \sum_{i=1}^{n} \frac{\sigma_i}{\alpha + \sigma_i^2} (\begin{bmatrix} A \end{bmatrix} \cdot \begin{bmatrix} u_i \end{bmatrix} \cdot \begin{bmatrix} v_i \end{bmatrix}$$
(7)

4.2 Methods for Testing Solution Schemes

Several different methods for obtaining the matrix \mathcal{M} from Eq. (2) have been considered. All of these methods are first tested with "perfect" input data. To generate this "perfect" input data, the direct problem is solved using known semianalytic solutions [3]. These solutions are based on solving Possio's integral equation for the pressure jump along a flat-plate airfoil in response to a three-dimensional gust. Equation (2) is then used to calculate the radiated sound. The far field is described on 79 equally space points on a circular arc, at r=100, from 0 to π but not including the endpoints. r is given in nondimensional units. The data are written out with eight decimal point precision.

4.3 Quadrature Method

A method commonly used for discretizing integral equations is to apply a simple quadrature rule. Hence, the first method tested, uses the trapezoidal quadrature rule to discretize Eq. (2). A reconstruction of the unsteady pressure jump on the airfoil is obtained by using the SVD method with imbedded Tikhonov regularization where $\alpha=10^{-7}$. The regularization method and parameter are chosen by running calibration cases for different Mach numbers and reduced frequencies. For a given solution scheme, once the choice is made, it must remain fixed for all other cases considered.

The dotted line in Figure 2, denoted Case A, shows the reconstruction for a case with M=.4 and $k_1=5.0$ when "perfect" input data are used. The figure includes the real and imaginary parts of the nondimensional unsteady pressure jump, $C_{\Delta p'}$. In the figure the leading edge of the airfoil is located at -1.0 on the airfoil axis and the trailing edge is located at 1.0. The reconstructions are not prefect even though "perfect"

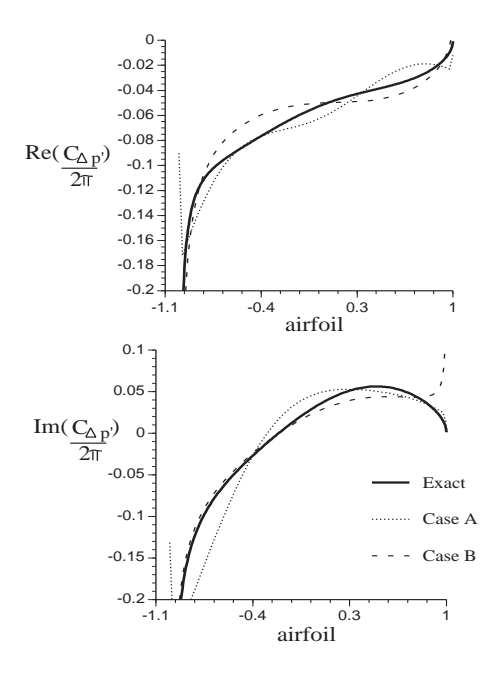


Figure 2: Comparison of reconstructions using the quadrature methods. $M=0.4, k_1=5.0$

input data have been used. The reconstructions becomes worse as $K = k_1 M/\beta^2$ decreases.

Most of the error in the reconstruction comes from the leading edge singularity behavior. Although this behavior is inherent in the problem, i.e., the information characterizes the kernel, computationally it is difficult to capture. Usually, computers do not handle singularities well; and, computations will damp out such behavior. In Figure 2, it can be seen that the solution grows as it progresses towards the leading edge but, it suddenly decreases right at the leading edge. This adds unwanted oscillations in the result.

To aid the numerics in capturing the leading edge singularity, the transformation $y_1 = -\cos\gamma$ is used. With this transformation, equation (2) becomes

$$P(\vec{x}) = \frac{-iK\tilde{x}_2}{4} X$$

$$\int_0^{\pi} \Delta P(\gamma) sin\gamma \frac{H_1^{(2)}(K|\vec{x} + cos\gamma\hat{i}|)}{|\vec{x} + cos\gamma\hat{i}|} d\gamma \qquad (8)$$

Solving the matrix equation for the quantity $\Delta P(\gamma) sin\gamma$ ensures that the computed quantity is finite at the leading edge. However, this might not yield $\Delta P=0$ at the trailing edge which violates the Kutta condition. This is not a real hindrance, however, since the reconstructions are very good except in a small region around the airfoil. This method is used for the case $M=.4,\ k_1=5.0$. The results are shown by the dashed line in Figure 2 and denoted Case B. Calibration for this method gives the Tikhonov parameter as $\alpha=10^{-6}$.

Overall, this method gives much better reconstructions but still they are not perfect. In particular, for small K, they are very poor. The reason for this difficulty can be traced to the relatively small dependence of the kernel phase on \tilde{y}_1 . Indeed, for large $|\vec{x}|$, $K|\vec{x}-\vec{y}|$ shows small variation as \tilde{y}_1 varies from -1 to 1. These variations become even smaller as K decreases. This is consistent with the fact that, as K becomes small, the far field does not depend on the details of the unsteady pressure which is well known from the compact source approximation.

The alternative, is to use the asymptotic behavior of the Hankel function to factor out the dependence on $|\vec{x}|$. Using the asymptotic form of the Hankel function, equation (2) can be written as

$$P(\vec{x}) \sim \sqrt{\frac{K}{8\pi}} \frac{e^{-i(K|\vec{x}|-\pi/4)}}{|\vec{x}|^{1/2}} sin\tilde{\theta} X$$

$$\int_{-1}^{1} \Delta P(\tilde{y}_1) e^{iK\bar{y}_1 cos\bar{\theta}} d\tilde{y}_1 + O(\frac{1}{|\vec{x}|^{3/2}}) \quad (9)$$

The integral equation to solve then, is

$$f(\tilde{\theta}) = P(\vec{\tilde{x}}) \sqrt{\frac{8\pi}{K}} e^{i(K|\vec{\tilde{x}}|-\pi/4)} \frac{|\vec{\tilde{x}}|^{\frac{1}{2}}}{\sin\tilde{\theta}}$$
$$= \int_{-1}^{1} \triangle P(\tilde{y}_1) e^{iK\cos\bar{\theta}\bar{y}_1} d\tilde{y}_1 \tag{10}$$

Again, we use the trapezoidal rule to discretize the matrix, and the transformation $y_1 = -\cos\gamma$ to avoid the difficulty associated with the leading edge singularity. Figure 3 shows the solution obtained from the SVD method with imbedded Tikhonov regularization when "perfect" input data are supplied. The regularization parameter for this method is $\alpha=10^{-6}$. These reconstructions are perfect and cannot even be detected on the plots since they lie directly on the solid curve for the exact solution. This method gives perfect reconstructions at all values of K that have been tested. These values range from .01 to 20. Because this method uses the asymptotic form of the kernel, it only works when the input data are taken in the far field.

In all of the reconstructions shown above, 79 far-field points lying between 0 and π were used. For smaller K cases, fewer points can be used. For instance, in the case shown here as few as 19 points can be used, corresponding to data locations eight degrees apart. This still may be too restrictive for application. Therefore either a higher order quadrature scheme or a collocation method must be used to transform the integral equation. Since a collocation series can be easily chosen to include the basic features of the unsteady pressure, this is the preferred method.

4.4 Collocation Method

The collocation series is chosen to include the square root singularity at the leading edge and the Kutta condition at the trailing edge, which are inherent in the problem. The collocation series is

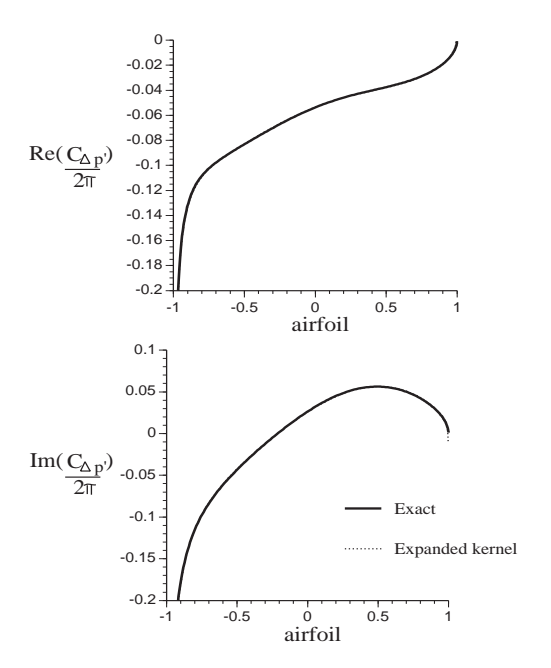


Figure 3: Reconstruction using the quadrature method with expanded kernel. $M = 0.4, k_1 = 5.0$

$$\Delta P(\gamma) = A_0 cot(\frac{\gamma}{2}) + \sum_{n=1}^{\infty} A_n sinn\gamma$$
 (11)

where $\tilde{y}_1 = -\cos\gamma$. This series can be used with the Hankel function kernel or with the expanded kernel, which adds flexibility in the sense that the input data can be obtained either in the mid field or in the far field. Substituting (11) into (10) and integrating gives

$$f(\tilde{\theta}) = A_0 \pi (J_0(K\cos\tilde{\theta}) - iJ_1(K\cos\tilde{\theta}))$$

$$+ \sum_{n=1}^{\infty} A_n \pi (-i)^{n-1} n \frac{J_n(K\cos\tilde{\theta})}{K\cos\tilde{\theta}}$$
(12)

where J_n is the Bessel function of order n. The Bessel functions have the property that

$$J_n(z) \sim \frac{1}{\sqrt{2\pi z}} \left(\frac{ez}{2n}\right)^n \text{ as } n \to \infty$$
 (13)

Therefore, the values of the elements in the columns of \mathcal{M} decrease as the column number increases. This leads to ill-conditioning again. However, the number of terms in the series can be limited such that the condition number of the matrix is closer to 1. This a priori regularization allows for direct inversion of the matrix. If the series is limited, however, most likely the system of equations will be overdetermined, which again hinders direct inversion. The system may be overdetermined since, even for large K cases, only about eight terms are needed in the series and most probably data will be available in the far field at more than

eight locations. The SVD method can be used to solve the overdetermined system. Since the regularization is done *a priori* an imbedded technique is not necessary.

The number of columns, i.e., terms used in the collocation series, is chosen based on the singular values. The restriction is that the singular values of the matrix must all be greater than the cut-off parameter .01. This parameter is chosen from calibration using "perfect" input data. It allows for perfect reconstruction for all cases of K, where .01 < K < 20. No figures are shown here, since the exact and reconstructed solutions coincide perfectly.

Although quadrature methods give good results, they require numerous far-field measurements. The collocation method has the advantage of requiring only a small number of input data which can be obtained from either the far field or the mid field. Depending on where the measurements are made, the corresponding kernel is used and the results are good for both kernels.

5. SENSITIVITY

We now examine the sensitivity of inverse methods to errors that exist in the measurements. Up until now, all of the discussion has assumed that the input data would be "perfect". In addition, the kernel used in calculating the input data is always identical to the kernel used for the inversion. We also note that, the far-field data have been generated numerically with great precision. It is no surprise, then, that in the end, methods which give perfect reconstructions are obtained. For application however, the far-field data will be obtained experimentally. This means that the data will contain nonlinear effects inherent to the acoustic propagation, noise from the surroundings, and measurement uncertainty due to the mechanical and electrical systems used to take the data. Therefore, it is important to show the robustness of the inversion method when the input is not "perfect". There are two sources of error in the current problem. One source is noise in the far-field data. This only affects the left hand side of (4). The second type of error comes from measurement errors of M and k_1 . These parameters affect the kernel itself, and therefore the matrix \mathcal{M} . The two different types of errors will be treated separately. First the sensitivity to input-data changes is treated.

5.1 The Third Hadamard Criteria

The third Hadamard criteria [2] for well-posedness of a problem, requires that the solution be continuously dependent on the data. This condition fails for the inverse aeroacoustic problem. In two dimensions, the relationship between the far-field pressure and the near-field pressure contains a factor of $1/\sqrt{r_f}$, where r_f is the distance to the far field. Because of this dependence, errors on the order of $\delta p'$ in the far-field input data becomes errors on the order of $\sqrt{r_f}\delta p'$ in the solution. Hence, small changes in the input data can create large changes in the solution, violating the third Hadamard criteria.

The ill-posedness of the inverse problem, manifests itself in the ill-conditioning of the matrix equation. The

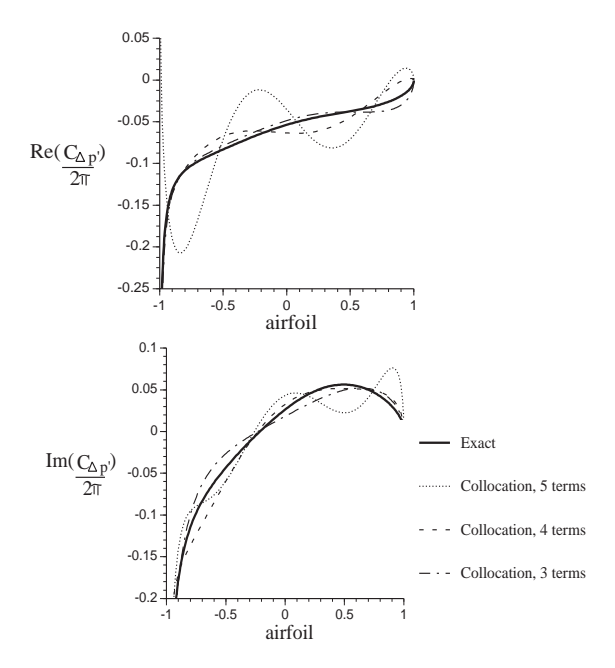


Figure 4: Reconstruction using the collocation method with truncated input data. Value of smallest singular value differs $M = 0.4, k_1 = 5.0$

sensitivity to errors in the input data and methods of controlling the sensitivity are discussed in the next few sections.

It is easy to see how this inherent magnification of error is produced by the solution method. Considering the singular value decomposition method shown in Equation (6), any errors in the input, A, will be magnified when dividing by small singular values. From this it is also clear how to control the sensitivity. A change in the choice of the regularization parameter must be considered. For the collocation method, the number of columns will be reduced so that the smallest singular value is 1.0. The new, $a\ priori$, cut-off parameter will not lead to perfect solutions when "perfect" input data are used, but the solutions are still very accurate.

To illustrate this point, input data, which have a maximum value of .3, are truncated to two decimal places. This essentially adds noise to the data. The reconstruction using the truncated input data is shown in Figure 4. The difference between the curves in Figure 4 is the number of terms used in the collocation series. A 5-term collocation series coincides with a cut-off parameter of .01. The reconstruction is not good. A 3-term collocation series coincides with a cut-off parameter of 1.0 and the reconstruction is much better. It is not perfect but it is the same reconstruction that is obtained when only 3 terms are used in the series and "perfect" data are available. This indicates that the scheme with a priori cut-off 1.0 is not as sensitive to errors in the input.

Truncating the data, helps to set the new cut-off parameter. For a more realistic study of the sensitivity of solutions to the far-field data sensitivity we now investigate how the reconstructions depend on the level of

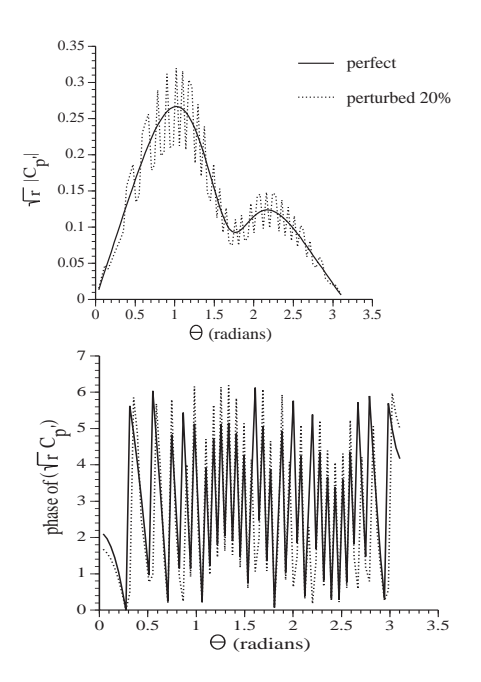


Figure 5: The 20% perturbed in put data. Top: magnitude. Bottom: phase. $M=0.4, k_1=5.0$

error in the input data. To this end, it is assumed that k_1 and M are known accurately. For every error analysis both the perfect input data and the noisy input data are shown as well as their respective reconstructions. Several methods for perturbing the input data will be used and the corresponding reconstructions shown.

5.1.1 Relative Error

The first type of error considered is a relative error. The magnitude and phase of the far-field data are both perturbed by $\pm 20\%$ at every measurement location. Using the collocation method with a priori regularization, the reconstructions are performed. The results are shown in Figures 5 - 6. In Figure 5, the solid line represents the "perfect" input data and the dotted line shows the erroneous input data. Both the magnitude and phase of the input are included. The reconstructions are shown in Figure 6. The results are not perfect, but for the amount of error in the input data, the reconstructions are reasonable.

5.1.2 <u>Uniform Error</u>

Rather than the error being a percentage of the data at a given location, often, the error is more uniform at all locations. Thus we consider errors made by uniformly perturbing the data. In this case, random numbers less that or equal to .1 are added or subtracted to the real and imaginary parts of the far-field data at every measurement location. The perturbed input data are shown in Figure 7 and the reconstruction can be found in Figure 8.

This reconstruction can be improved. The improvement is based on the fact that any error in the data at measurement locations directly upstream and directly downstream of the flat-plate airfoil will be amplified due to the division by $sin\tilde{\theta}$. Instead of using data

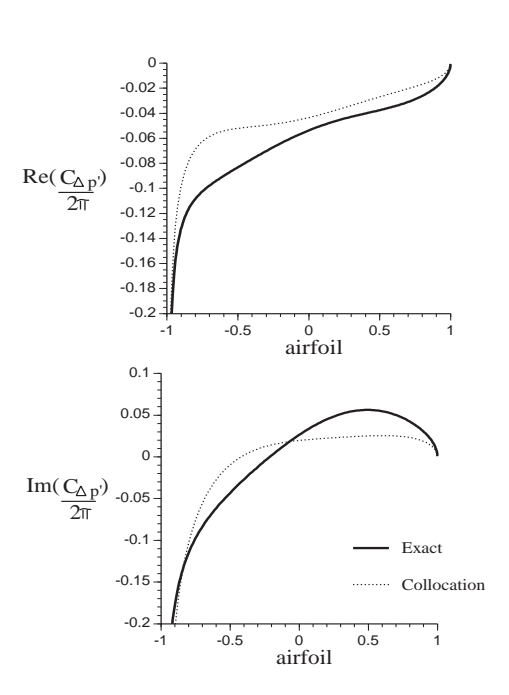


Figure 6: Reconstruction using the collocation method with "20% perturbed" input data. $M=0.4, k_1=5.0$.

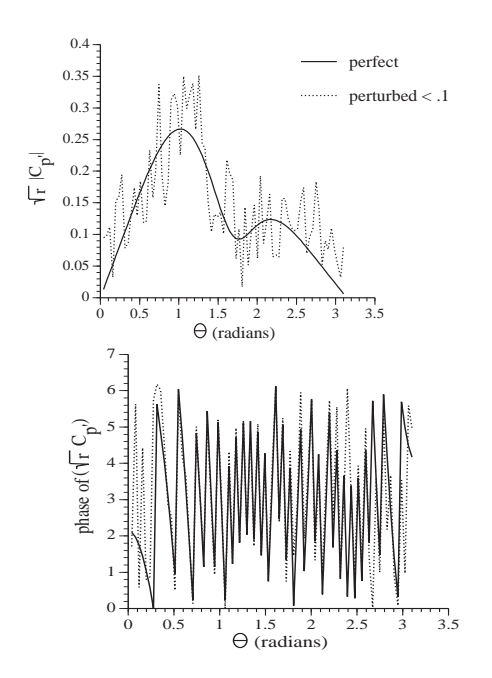


Figure 7: The "uniformly perturbed" input data, changes less than .1. Top: magnitude. Bottom: phase. $M = 0.4, k_1 = 5.0$.

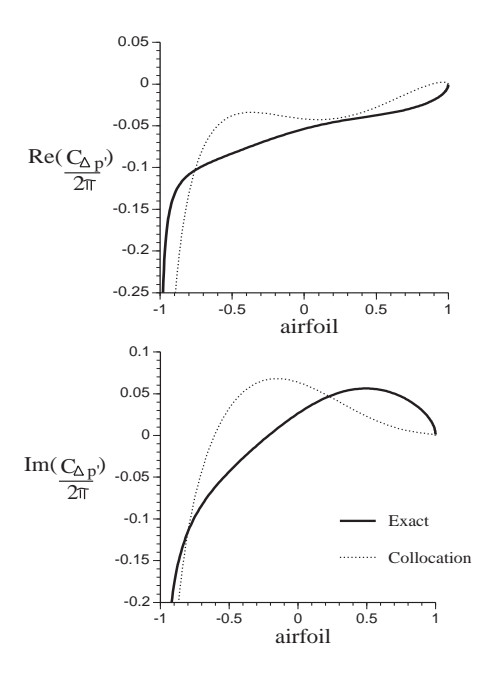


Figure 8: Reconstruction using the collocation method with "uniformly perturbed" input data, changes less than .1. $M=0.4, k_1=5.0$.

locations on an arc from 0 to π , the arc is restricted from $\pi/8$ to $7\pi/8$. The reconstruction is shown in Fig. 9 and the improvement is significant. Neglecting the measurements upstream and downstream is consistent with experiments, since often a flow inlet and outlet are located directly upstream and downstream respectively.

5.1.3 General Bias

A general bias error is the last type of error considered. Here the magnitude of the input data is increased by .05 everywhere. This type of error simulates a possible calibration bias in an experimental setup. The reconstructions seen in Figure 11 are poor when all the data are used. On the other hand, when the upstream and downstream data are removed, these reconstructions are improved. Figure 12 shows the improved results.

5.2 Sensitivity to Frequency and Mach Number

The far-field pressure is not the only input for the inverse problem. Other inputs include k_1,k_3 , and the Mach number. These parameters combine to give the value of $K=\sqrt{\frac{k_1^2M^2}{\beta^4}-\frac{k_3^2}{\beta^2}}$ which is a parameter in the kernel. These parameters are also used in the Reissner transformation, $P=p'e^{iMK_1\bar{x}}$, which helps to transform the governing equations into the Helmholtz equation.

The sensitivity of reconstructions to errors in these parameters is first demonstrated by increasing the Mach number 5%. Figure 13 shows the far-field data for the cases $M=.4, k_1=5.0$ and $M=.42, k_1=5.0$. The reconstruction is found using the input data corresponding to $M=.42, k_1=5.0$ but the input parameters of $M=.4, k_1=5.0$. the results are given

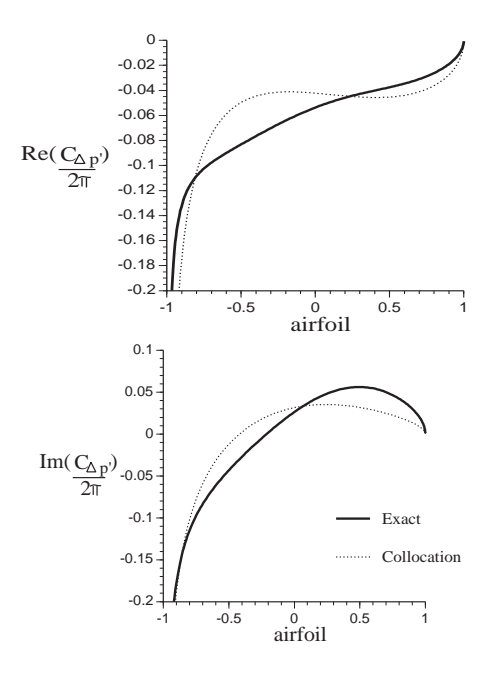


Figure 9: Reconstruction using the collocation method with "uniformly perturbed" input data, changes less than .1. Neglecting upstream and downstream data. $M=0.4,\,k_1=5.0.$

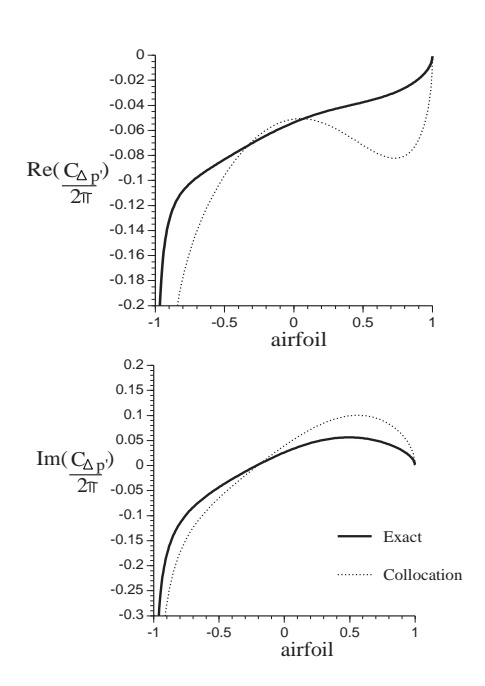


Figure 11: Reconstruction using the collocation method with input data with magnitude .05 larger than it should be. $M=0.4, k_1=5.0$.

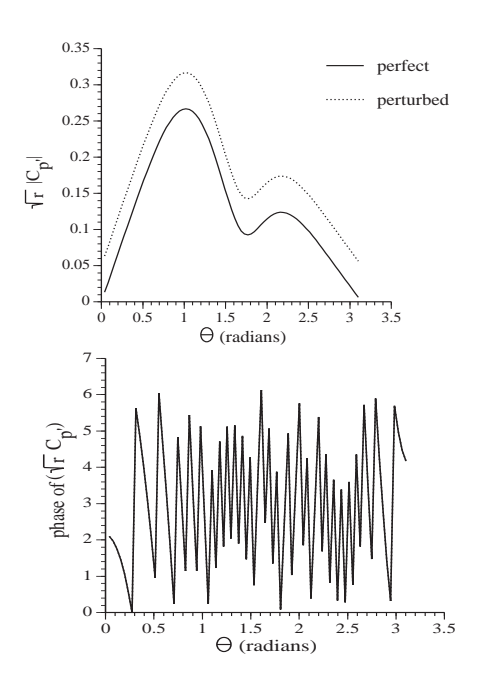


Figure 10: Input data when the magnitude is uniformly increased by .05. Top: magnitude. Bottom: phase. $M=0.4, k_1=5.0.$

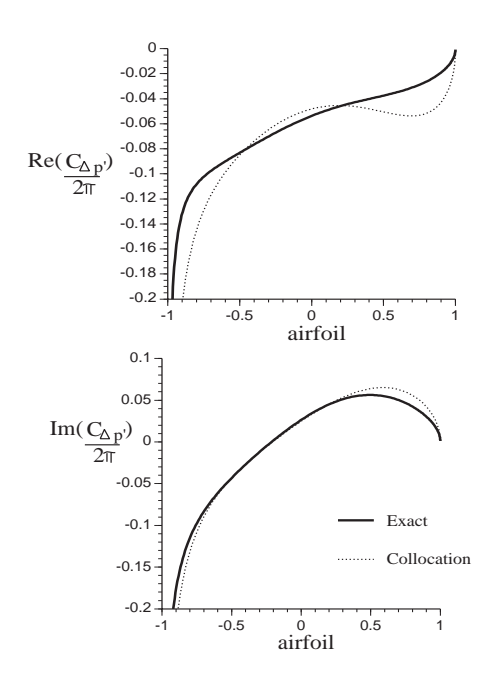


Figure 12: Reconstruction using the collocation method with input data with magnitude .05 larger than it should be. Neglecting data upstream and downstream. $M=0.4, k_1=5.0$.

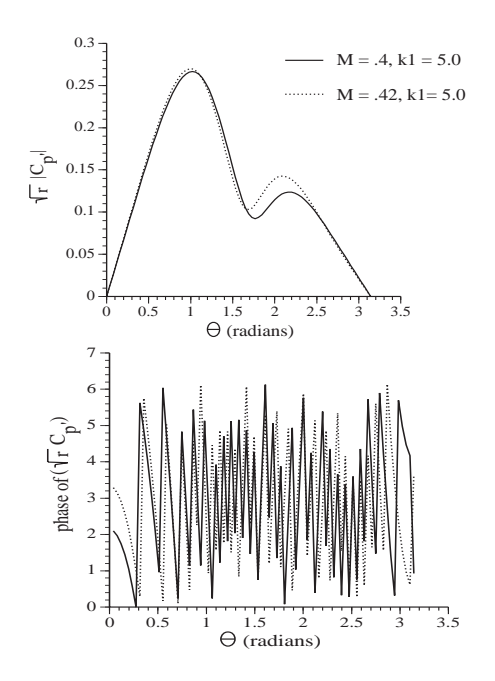


Figure 13: Magnitude and phase of far-field data for $M = 0.4, k_1 = 5.0$ and $M = 0.42, k_1 = 5.0$.

by the dotted line in Figure 14.

In a second example, the reduced frequency is increased by 5%. Figure 15 shows the far-field data for the cases $M=.4, k_1=5.0$ and $M=.4, k_1=5.25$. The reconstruction determined from input data corresponding to $k_1=5.25$ but input parameter $k_1=5.0$ is found in Figure 16. Again the reconstruction is not accurate. Changing the regularization parameter, or using the quadrature methods do not improve the reconstructions

5.2.1 Far Field vs. Mid Field

At large distances the asymptotic form of the kernel includes the term $e^{iK\bar{r}}$. Therefore, when \tilde{r} is very large, any error in K is significantly amplified. Since magnification of the errors in K is due to the location of the measurement surface in the far field, such large reconstruction errors should not occur if the measurements are made in the mid field. This corresponds to r on the order of 10. The reconstructions when r=10and r = 5 for the previous two examples are shown in Figures 14 and 16. Some improvement can be seen. In other cases tested, errors in the input parameters on the order of 1%, when the input data are taken at r = 10, do not affect the reconstruction significantly. Errors larger than 1% however, do alter the reconstructions. There is a possibility that the optimization scheme could be extended to find an optimal value of K, but at this point this is an open problem. So if this method is to be used in application, the measurement of these quantities needs to quite accurate.

7. CONCLUSION

The inverse aeroacoustic problem associated with a gust impinging on a flat-plate airfoil is formulated in

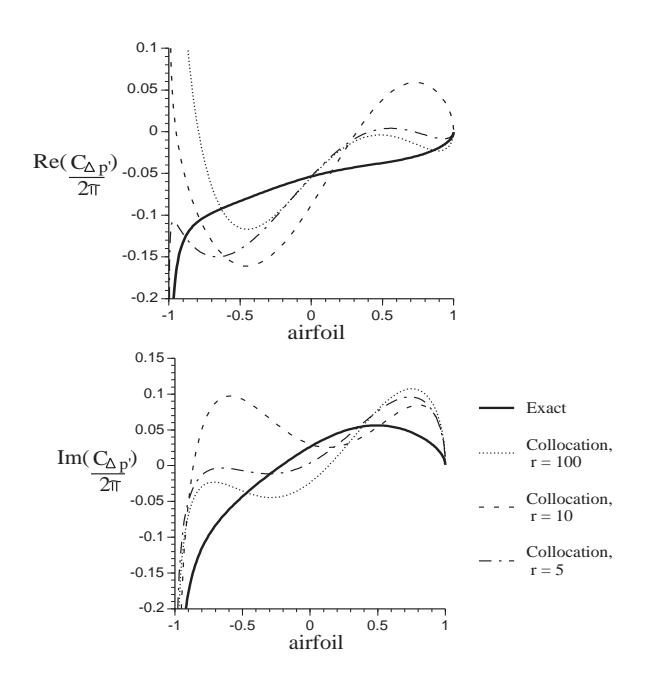


Figure 14: Reconstruction using input parameters, $M = 0.4, k_1 = 5.0$ but input data corresponding to $M = 0.42, k_1 = 5.0$ at r = 100, r = 10 and r = 5.0

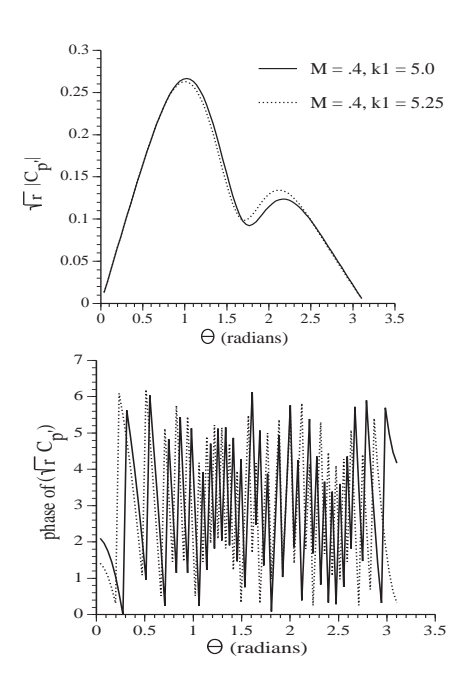


Figure 15: Magnitude and phase of far-field data for $M=0.4, k_1=5.0$ and $M=0.4, k_1=5.25$.

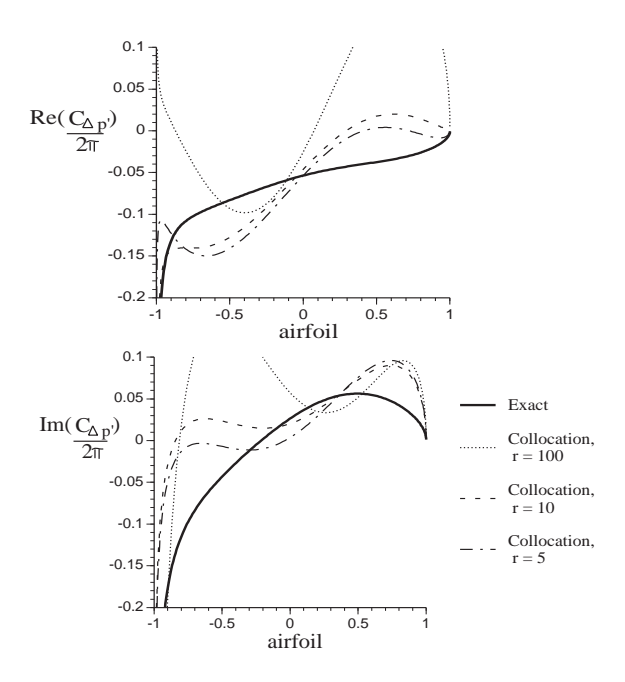


Figure 16: Reconstruction using input parameters $M = 0.4, k_1 = 5.0$ but input data corresponding to $M = 0.4, k_1 = 5.25$ at r = 100, r = 10 and r = 5.0

terms of a Fredholm integral equation of the first kind. The feasibility of determining the unsteady pressure along the airfoil surface from the radiated acoustic signal is demonstrated. The ill-posedness associated with the third Hadamard condition, results in an illconditioned algebraic system of equations. This system of equations is solved using the method of singular value decomposition with regularization. Discretization and collocation techniques were used to represent the unsteady pressure on the airfoil surface. In the discretization method, the accuracy of the inversion process is improved by a transformation which helps capture the leading edge singularity in the unsteady pressure on the airfoil surface. Moreover, to avoid the difficulties associated with the large phase variation of the acoustic signal, the kernel of the Fredholm integral equation is expanded and the term causing the large phase variation is factored out. This approach, in conjunction with the transformation, gives very accurate reconstructions when "perfect" input data are used. Alternatively, a collocation technique was developed, which embodies the characteristics of the unsteady pressure along the airfoil surface such as the leading edge singularity and the Kutta condition at the trailing edge. The collocation technique also gives very accurate reconstructions when "perfect" input data are used. The collocation technique has the added flexibility of working well with either the regular kernel form or its far-field asymptotic expansion. As a result, both far-field and mid-field input data can be used. The most attractive feature of the collocation technique is that it requires input data from very few far-field loca-

Various sensitivity analyses are implemented to determine the practical feasibility of the reconstruction. These included: relative, uniform, and biased errors in the input data. The results show that the sensitivity of the inverse solution to errors in the input data can be controlled by an optimal choice of the regularization parameter. A similar sensitivity analysis of the effect of mean-flow parameters, M and k_1 , shows that the use of mid-field data produces a significant improvement in the reconstructions.

ACKNOWLEDGEMENTS

The research was supported by the Office of Naval Research Grant No. N00014-92-J-1165 and monitored by Mr. James A. Fein. Sheryl M. Patrick would like to thank Zonta International for their partial support.

REFERENCES

- [1] Atassi, H. M., (1994), "Unsteady Aerodynamics and Vortical Flows: Early and Recent Developments," Aerodynamics and Aeroacoustics, Editor K. Y. Fung, Chap. 4, pp. 121-171, World Scientific.
- [2] Hadamard, J., (1923), Lectures on Cauchy's Problem in Linear Partial Differential Equations, Yale University Press, New Haven, Conn.
- [3] Atassi, H. M., Dusey, M. and Davis, C. M., (1993), "Acoustic Radiation from a Thin Airfoil in Nonuniform Subsonic Flow," AIAA Journal, Vol. 31, No. 1, pp. 12-19.
- [4] Patrick, S. M., (1995), "An Inverse Problem For a Nonuniform Subsonic Flow Interacting With A Body And Radiating Sound," Ph.D. Thesis, University of Notre Dame, Notre Dame, Indiana.
- [5] Patrick, S., M., Atassi, H. M. and Blake, W. K., (1994) "Inverse Problems in Aerodynamics and Aeroacoustics," Active Control of Vibration and Noise, ASME DE-Vol. 75, November 1994, pp. 309-319.
- [6] Tikhonov, A. N., (1963), "Regularization and Incorrectly Posed Problems," Soviet Mathematics, Vol. 4, no. 6, pp. 1624-1627. (English translation).